ATTENUATION OF SURFACE WAVES IN DEEP WATER

by

Michael Stuart Carswell

UNITED STATES
NAVAL POSTGRADUATE SCHOOL

THESIS

ATTENUATION OF SURFACE WAVES IN DEEP WATER

by

Michael Stuart Carswell

December 1968

ATTENUATION OF SURFACE WAVES IN DEEP WATER

by

Michael Stuart Carswell
Lieutenant Commander, United States Navy
B. S., Purdue University, 1956

Submitted in partial fulfillment of the
requirements for the degree of

MASTER OF SCIENCE IN OCEANOGRAPHY

from the

NAVAL POSTGRADUATE SCHOOL
December 1968

ABSTRACT

The concept, instrumentation, and analytical techniques for the investigation of attenuation of wind generated water surface waves in a small scale real environment by separation of generation and propagation by time in the dying wind situation were developed, and an empirical attenuation function applicable to a wide range of frequencies proposed.

TABLE OF CONTENTS

LIST OF TABLES

LIST OF ILLUSTRATIONS

TABLE OF SYMBOLS AND ABBREVIATIONS

Symbol	Definition	Units
$A(t_k)$	discrete wave amplitude in time domain	mm.
$\hat{A}(f_j)$	complex Fourier amplitude	mm.
$\hat{A}^*(f_j)$	complex conjugate of $A(f_j)$	mm.
B_e	equivalent bandwidth, M Δf	sec^{-1}
C	arbitrary constant	
COMCOR	Computer Corporation	
DIA	diameter	in.
$f_j = j \Delta f$	a discrete frequency	sec^{-1}
f_c	aliasing or Nyquist folding frequency	sec^{-1}
f	frequency	sec^{-1}
ft	feet	
g	acceleration of gravity	$ft\text{-}sec^{-2}$
G(f,x)	attenuation function	
GALV.	Galvanized	
HARM	IBM computer library subroutine for fast Fourier transform	
H(f,x)	an error function	
Hz	Hertz, cycles per second	sec^{-1}
i	$\sqrt{-1}$	
in	inches	
IBM	International Business Machines	
j	frequency index	
k(x,θ,f)	angular spreading function	
K	attenuation constant	sec^p/nm
k	time index	
LB	pound, unit of force	

°(M)	degrees magnetic	
m, m(f), $m(f_j)$	attenuation coefficient	ft^{-1} or nm^{-1}
MWL	mean water level	
Mfd	microfarad, unit of capacitance	
M	number of elementary bands in B_e	
mm	millimeters	
N	number of sample points	
nm	nautical miles	
Ω	ohms, unit of resistance	
p	an integer	
P(f,x)	a predicted energy density spectrum	mm^2-sec
π	ratio of circumference of circle to diameter	
R(f,x)	P(f,x)/ S(f,x)	
RMS	root mean square	
SDS	Scientific Data Systems	
S(f,x)	continuous energy density spectrum at a propagation position	mm^2-sec
S(f,0)	continuous energy density spectrum at a generation position	mm^2-sec
$S(f_j)$	average energy density in bandwidth B_e	mm^2-sec
sec	seconds	
Sig.Gen.	signal generator	
$t_k = k \Delta t$	a discrete time	sec
Δt	sample interval	sec
t	wave propagation time at group velocity	sec
T_r	length of wave record	sec
θ	range of possible directions through which waves in a fetch can propagate to a down-wind point of interest	

θ_3, θ_4	limits of θ	
VAR.	variation	degrees
V_g	group velocity	$ft\text{-}sec^{-1}$
x	separation of two points along axis of wave propagation	ft
"	inches	
	diode	
	transformer	
	capacitor	
	resistor	
	alternating current source	
	ground potential	

ACKNOWLEDGEMENTS

The author extends his sincere appreciation to Professor J. B. Wickham, under whose guidance this project was accomplished, for his patience, advice and encouragement; to Mr. R. L. Limes, Supervisor, Electrical Engineering Department Computer Laboratory, for making available the SDS 9300-COMCOR 5000 hybrid computer system and for the time he devoted to insuring successful analog to digital conversion of the data used in this study; to Lieutenant Jerry L. Post for his newly developed high-speed sampling and conversion programs; and to the Public Works Street Maintenance Department, City of Seaside, California, who provided electrical power for the wave recording equipment during many long hours of waiting for the wind.

I. INTRODUCTION

The concept of wind-driven ocean waves as spectra of harmonic components which follow the laws of linear hydrodynamics was introduced in 1948 by Barber and Ursell (1). There has since been considerable progress toward the mathematical and physical description of ocean wave processes, with the ultimate objective being the prediction with reasonable certainty of future wave conditions at any geographical point on the basis of worldwide synoptic observations of both wave and wind fields. A summary of the major contributions to knowledge of ocean waves was compiled in 1967 by Cartwright (2).

While theoretical models of wave generation, dispersion and geometrical spreading have been fairly well confirmed empirically and are used as the current basis of wave forecasting, the attenuation of waves during propagation is less well understood; and an attenuation function is consequently not applied in many wave-forecasting techniques.

Some classical theories of wave attenuation, namely air resistance and turbulent friction, were critically examined by Darbyshire (4) and found wanting as singular explanations. The theory of non-linear scattering proposed by Phillips (6) appears promising and has been reasonably supported by Snodgrass, et. al. (11). Conceivably, the answer may lie in a combination of these processes.

As has been the case in studies of other environmental processes, it appears that the phenomenon under consideration must be completely described empirically before the question of theory can be resolved. So far, environmental studies of attenuation have been confined to low frequency ocean swell, where the range of measurable frequencies is

included in only one of several logarithmic decades of possible surface wave frequencies. The classical theories and the generalized model developed later in this paper call for the attenuation function to be exponential in propagation distance and frequency dependent. When the generalized model is applied to ocean wave statistics, the data are scattered within such a small band of the frequency scale that functions supporting almost all proposed theories can be fitted equally well to the data.

Accordingly, the primary objective of this research was the collection of attenuation data in a small scale real environment where the measurable frequencies are considerably displaced from those normally measured in ocean swell in order to give better definition to the attenuation function. This requirement for collection of data gave rise to the second objective, the development and evaluation of a system for recording and analyzing waves in a small scale real environment.

II. CONCEPTS

A. COMPARISON OF ENVIRONMENTS

Ocean wave attenuation studies involve the measurement of the energy of the relatively low frequency components of swell propagated over long distances from the area of generation. It is known that these low frequencies required high winds of appreciable duration for their development, hence the source of the swell waves can be located with fair accuracy in relation to the distance from the measuring instrument. A knowledge of wind or pressure conditions in the fetch can provide a reasonable estimate of the energy of waves in the fetch.

High frequency waves can be generated by the prevailing low velocity winds which are normally found over most of the ocean surface. For this and other reasons of distance and instrumentation, it would be extremely difficult to make meaningful measurements of these frequencies with sufficient precision in the ocean to determine attenuation. For purposes of this paper, high frequencies shall be defined as those frequencies approaching, but not including, frequencies in which surface tension is the predominant restoring force rather than gravity.

A lake or non-tidal estuary of moderate depth provides an ideal facility where experimental control is possible in the comparative measurement of high frequency deep water waves, although the scale of wind circulation in relation to the size of the lake or estuary provides no geographical separation between areas of generation and non-generative propagation. On this scale, however, the mean wind may change rapidly in speed and/or direction. In a case where the wind speed diminishes rapidly, some frequencies generated at the higher wind speed

would receive no more energy and would propagate as swell. This concept, that fetch and swell can be separated by time just as there is the geographical separation in the ocean, is a fundamental assumption of this paper.

B. THE GENERALIZED ATTENUATION FUNCTION

Let $S(f,x)$ represent the energy density spectrum computed from a wave record at a downwind (propagation) position, and let $S(f,0)$ represent the energy density spectrum computed from a wave record at an upwind (generation) position, where f is the component frequency and x is the separation between two points of measurement along the axis of maximum propagation (the direction of the mean wind during generation). Then,

$$S(f,x) = S(f,0) \quad k(x,\theta,f) \quad G(f,x) \tag{1}$$

where $G(f,x)$ is the attenuation function, and $k(x,\theta,f)$ denotes what portion of $S(f,0)$ would reach the downwind position if no attenuation were involved. This is a function of geometry and the beam pattern in the generating area. In this paper the model of Pierson, Neumann and James (9) will be used, where for all f

$$k(x,\theta,f) = \frac{2}{\pi} \int_{\theta_3}^{\theta_4} \cos^2 \theta \, d\theta \tag{2}$$

The angles θ_3 and θ_4 are measured at the edges of the fetch from the direction of the axis described above to the direction of the downwind measurement point.

Let $P(f,x)$ be a prediction of the spectrum at the downwind position which has not allowed for attenuation. Then,

$$P(f,x) = S(f,0) \quad k(x,\theta,f) \quad H(f,x) \tag{3}$$

where H(f,x) is an error function accounting for possible statistical errors in measurement at the upwind and downwind positions, and includes differences between the angular spreading model and the actual angular spreading phenomenon. The model has proved to be fairly representative of actual geometrical spreading, and H(f,x) should be at most a very slowly changing function of x. The spacial variation of H is thus ignored.

Divide (3) by (1)

$$R(f,x) = \frac{P(f,x)}{S(f,x)} = \frac{H(f,x)}{G(f,x)} \tag{4}$$

Differentiate

$$R'(f,x) = \frac{dR}{dx} = -H(f,x) \frac{G'(f,x)}{G^2(f,x)} \tag{5}$$

Substitute (4) in (5)

$$R'(f,x) = -R(f,x) \frac{G'(f,x)}{G(f,x)} \tag{6}$$

Now, assume that R(f,x) can be represented by:

$$R(f,x) = C\, e^{mx} \tag{7}$$

where m = m(f), and C is a constant. This assumption appears to be valid from empirical data in ocean swell studies over a wide range of x. Differentiating (7) and substituting (7) in the result,

$$R'(f,x) = Cm\, e^{mx} = m\, R(f,x) \tag{8}$$

then substitute (8) in (6), and

$$G'(f,x) = -m\, G(f,x) \tag{9}$$

which is a simple differential equation with solution

$$G(f,x) = G_o(f,0)\, e^{-mx} \tag{10}$$

Clearly, at the upwind measuring position, the function $G_o(f,0) = 1$ and

$$G(f,x) = e^{-mx} \tag{11}$$

The attenuation coefficient m is a function of frequency and environmental conditions. Empirical evidence indicates that it increases with frequency, and from physical considerations it should reasonably increase from following wind to opposing wind conditions. Other environmental conditions may also be important.

III. INSTRUMENTATION

Two resistance wave meters, adapted from a design by Pearlman (5), were constructed and used to collect data for this paper. A schematic diagram of the circuit used in both meters is shown in Figure 1.

Pearlman's paper demonstrated that this type of wave sensor is essentially linear over a range of wave heights of a few inches in static and vertical oscillation tests and has errors of less than one percent when tested in orbital motion. Static tests of the modified design used in this research confirmed the linear characteristics of the instruments.

The fixed resistors in the wheatstone bridge were standard 5% tolerance resistors, but were matched by measurement on a resistance bridge to have values within 0.5 ohm of the resistance shown. The variable resistor was used to null the bridge at an initial immersion in the field prior to recording data.

The signal generators used were Hewlett Packard Model 2000 audio oscillators. The recorder was a 14 channel Ampex CP-100 tape recorder. As the signal generators and the tape recorder both have one grounded terminal, the isolation transformer was required to prevent grounding one leg of the wheatstone bridge.

Alternating current was used to minimize electrolytic effects on the electrodes. The full wave rectifier shown in Figure 1 demodulated this carrier frequency, passing a direct current signal to the recorder that varied in response to the waves. The signal generators were operated at 3 volts (RMS) at about 2000 Hz; however, when operating two wave meters on one recorder, it was necessary to have about 150 Hz difference in the output of the signal generators to prevent a beat frequency from interfering with the wave records.

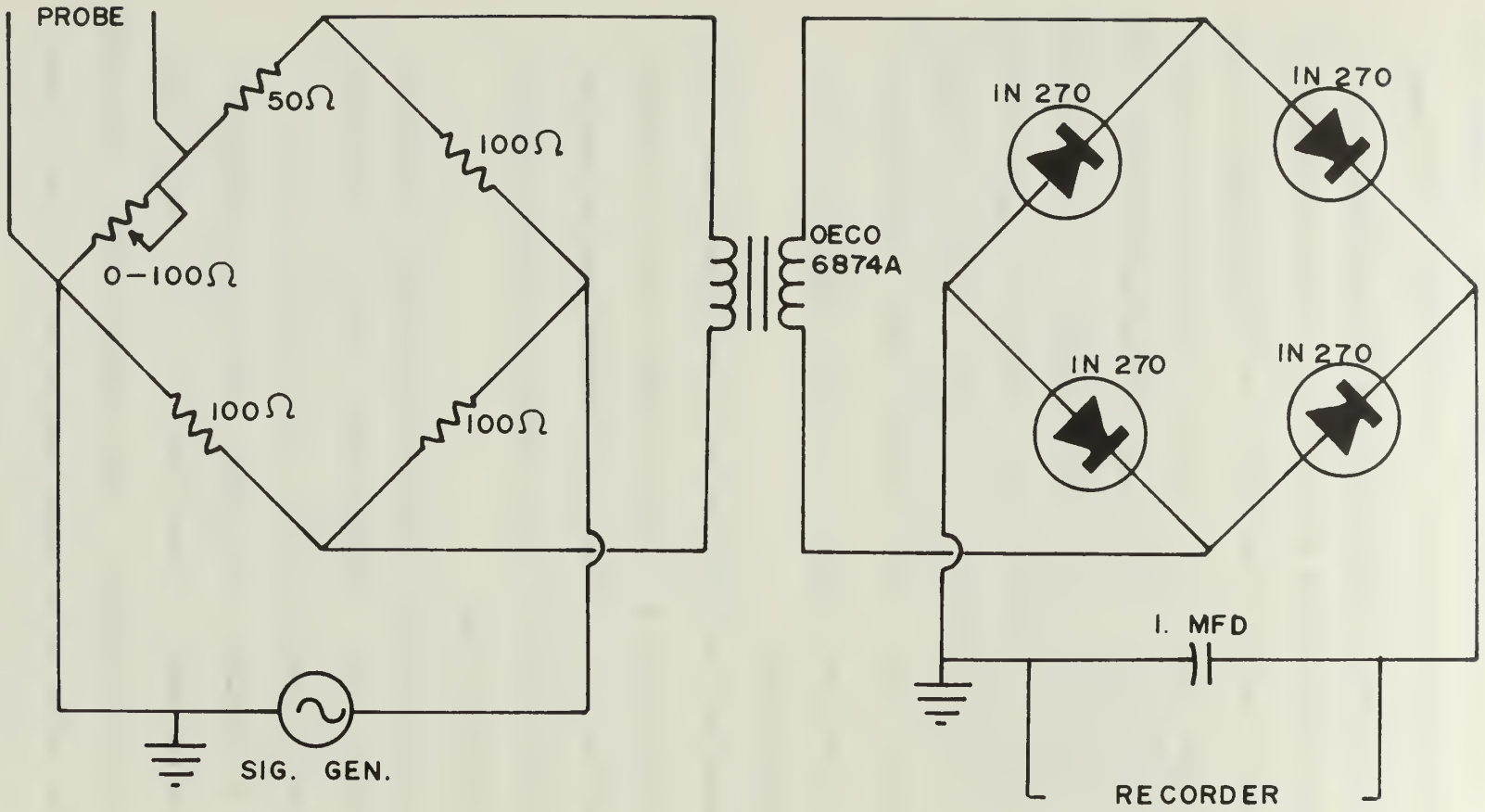

FIGURE 1. SCHEMATIC OF WAVE METER CIRCUIT

A dual beam oscilloscope was used to monitor the input and output of the tape recorder to insure proper recording of the wave signal. The 1 Mfd capacitor used across the rectifier output matched the input impedance of the tape recorder and oscilloscope, but the use of other equipments with different input impedances would require a change in capacitance to provide a smooth rectifier output without attenuating wave frequencies.

The Ampex CP-100 tape recorder was operated with frequency modulation recording and reproducing amplifiers for the wave record channels at a tape drive speed of 1-7/8 inches per second. A third channel was used with amplitude modulation (direct) amplifiers for a voice time record.

Details of the sensing probes are shown in Figure 2. The frames were designed to provide adequate rigidity, yet to minimize turbulence and reflections. The lower horizontal supports were designed to be at a depth greater than one-half wavelength of the anticipated waves. The fishing line shown was used as an insulator and to minimize the amount of electrode wire immersed. If the electrodes had extended to the lower horizontal support, the wheatstone bridge could not have been brought to near-balance by the variable resistor. In practice, it was found that the bridge could be nulled at an electrode immersion of no more than 2 centimeters.

The probe frames were attached to 1 inch diameter galvanized pipes driven into the lake bottom by means of the 1¼ inch diameter sleeves shown in Figure 2. The meter circuits were mounted on top of the frame and connected to the oscillators and recorder ashore with Alpha #2311 low capacitance shielded microphone cable laid on the bottom.

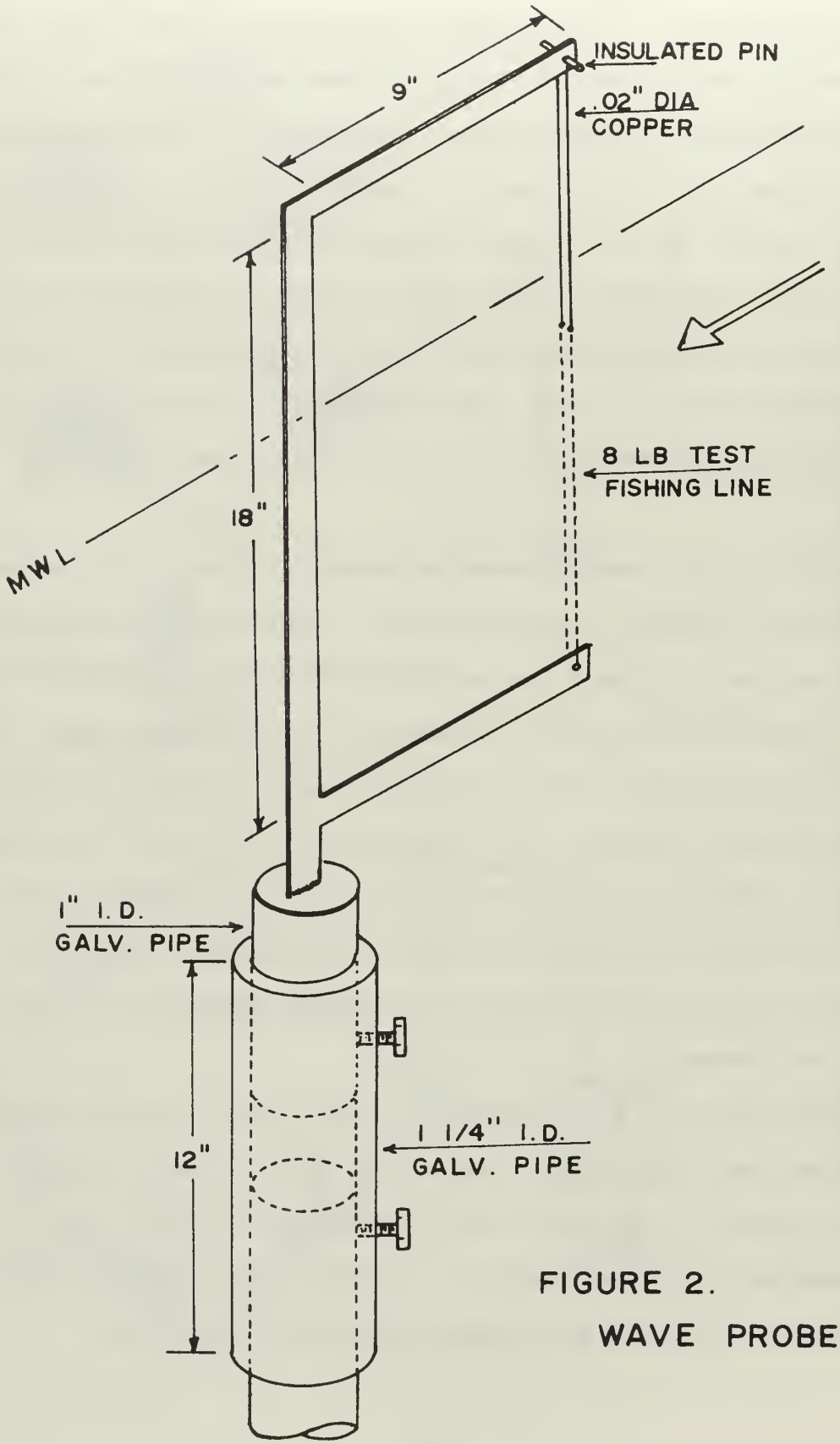

FIGURE 2.
WAVE PROBE

IV. DATA COLLECTION

Roberts Lake, 1500 feet from Monterey Bay in Seaside, California, was used for the collection of data in support of this paper. The lake, shown in Figure 3, is uniformly 5 to 5½ feet deep, with a soft mud bottom. Dense reed growth in the water around the circumference minimizes wave reflections.

The Monterey Bay area was considered suitable for this small scale attenuation study because its climatological characteristics are favorable to sudden changes in the wind. In addition to unpredictable changes in the wind field, diurnal heating and cooling of the Salinas Valley 20 miles inland results in a sea breeze during the day which dies suddenly at dusk. This general characteristic is modified or not apparent when the central California coast is under the influence of transient high or low pressure regions. In three weeks of daily attempts to collect data, only one day produced the desired rapidly dying wind.

Two sets of data, identified as data sets A and B, were collected on 21 November 1968. The wind speeds, as measured with a Casella precision anemometer mounted eight feet above the lake surface, are shown in Figures 4 and 5. The Casella anemometer provides a mean wind speed by recording the revolutions of a three cup rotor on a digital counter. The wind data in data set A, Figure 4, were recorded for one-minute averages, and in data set B, Figure 5, for half-minute averages.

Details of wave sensor placement are shown in Figure 3. For data set A, the sensing probes were on an axis of 230°(M). Although the actual distance between probes was 400 feet, the direction of the wind (from 300°(M)) reduced the effective propagation distance to 138 feet. For data set B, the probes were 120 feet apart on an axis of 290°(M).

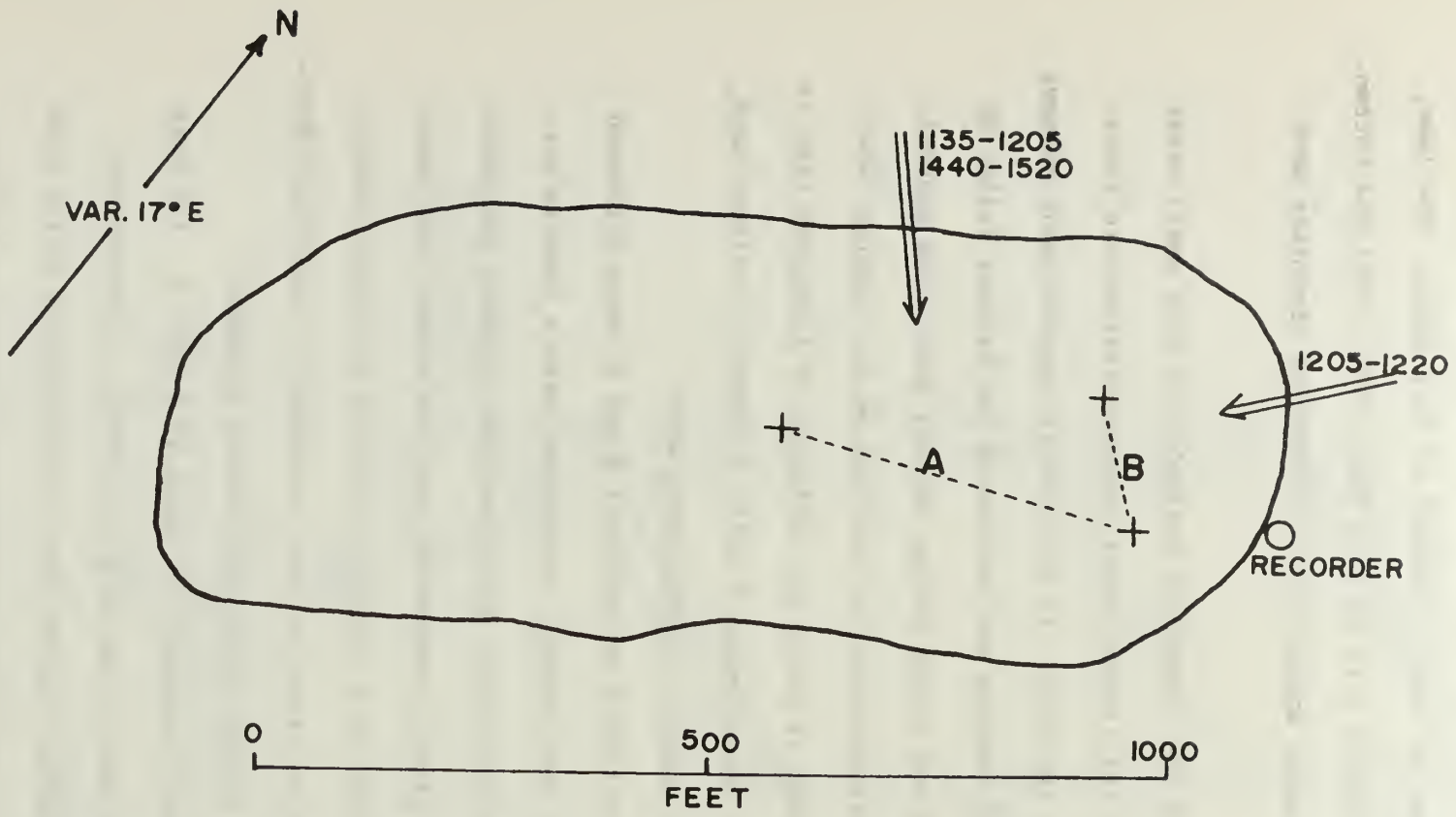

FIGURE 3. ROBERTS LAKE

Prior to collecting the wave data, both probes were immersed simultaneously in relatively still water near the edge of the lake at two levels of immersion and one minute recordings of the signals were placed on magnetic tape for calibration of the wave meters. The average values of the one minute calibration signals were later used to scale the wave records to actual amplitudes in millimeters.

FIGURE 4. WIND RECORD FOR DATA SET A

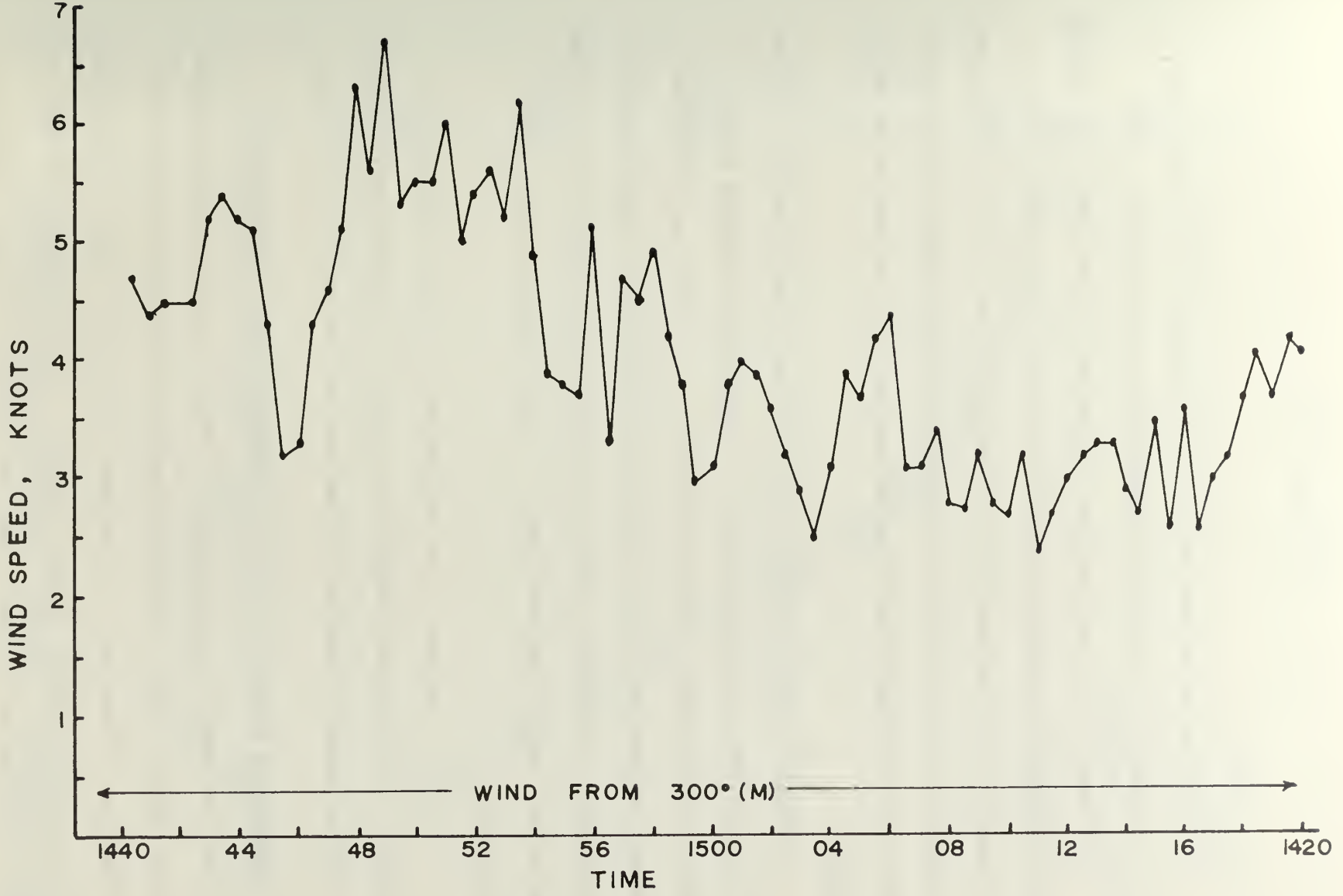

FIGURE 5. WIND RECORD FOR DATA SET B

V. ANALYSIS OF DATA

A. DIGITIZING

The calibration records and selected portions of the wave records were digitized with an SDS 9300-COMCOR 5000 hybrid computer system.

The Ampex CP-100 tape recorder was patched to the COMCOR 5000 analog computer through operational amplifiers included in the logic board of the computer and a low pass filter constructed from logic board components. The amplifiers were adjusted to amplify the maximum signal on the magnetic tape record to slightly less than the maximum input voltage of the analog computer.

A schematic diagram and plot of the measured characteristics of the low pass filter are shown in Figure 6. To minimize aliasing in later spectral calculations, 128 Hz was selected as a filter cut-off frequency. Although frequencies of that order were far beyond the range of expected surface wave frequencies, noise could possibly have existed in that range from either inherent equipment noise or beats between the wave meter oscillators.

To provide a minimum of two samples per cycle up to the cut-off frequency, the record was sampled at a rate of 256 samples per second. The digital computer sampling program used was developed by Post (10).

B. CONVERSION OF DATA FOR IBM 360 COMPUTER SYSTEM COMPATIBILITY

The core capacity of the SDS 9300 computer used for digitizing the data was far too small for spectral analysis of the wave records (see next section). Therefore, use was made of the much larger core capacity of the available IBM 360 computer system. The two computers do not share common symbology and storage parameters; however, a program developed by

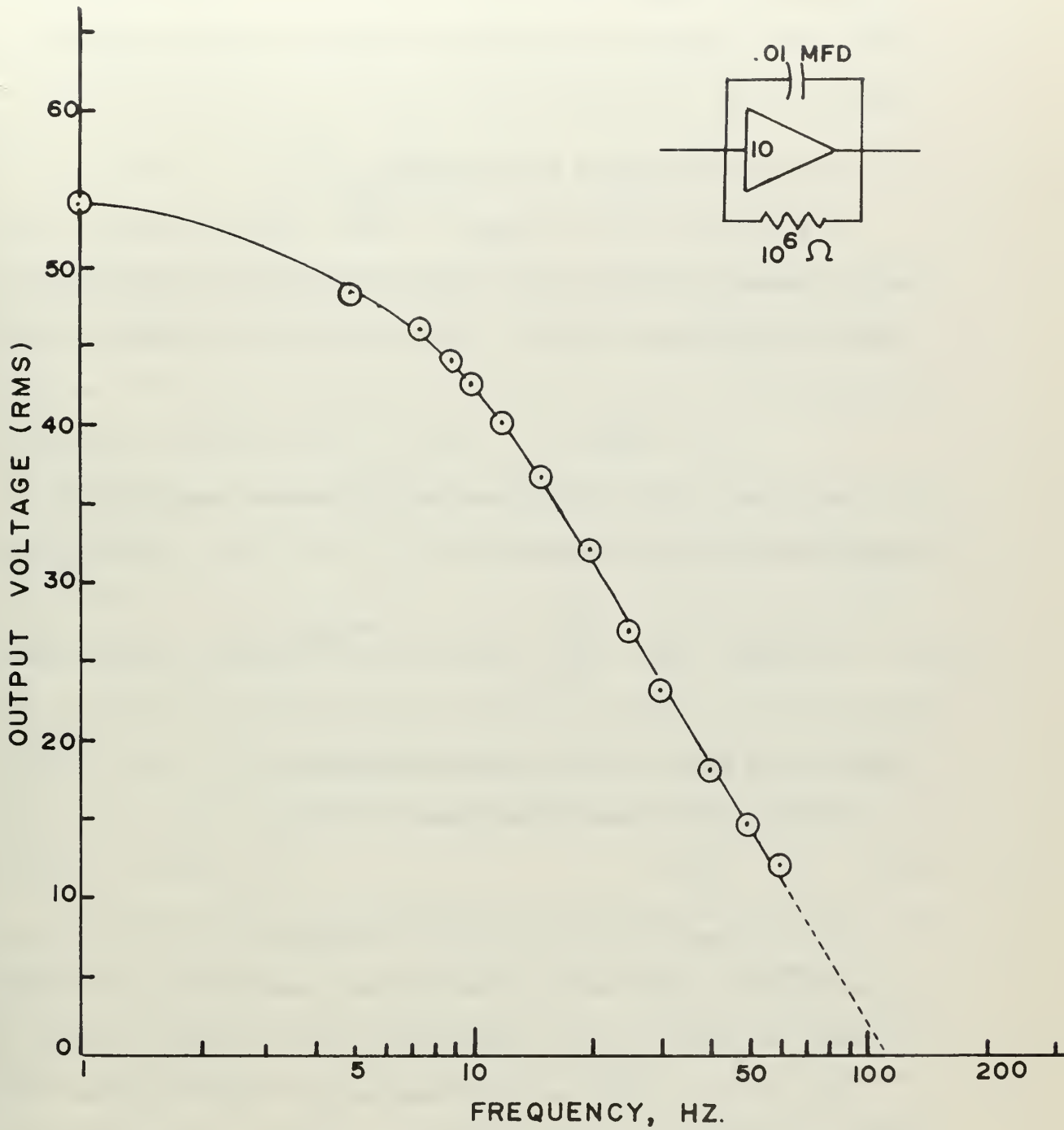

FIGURE 6. ANALOG FILTER CHARACTERISTIC

Post (10) for conversion of data from one system to the other was used to transfer and convert the digitized data from the tape record made on the SDS 9300 computer to a tape record compatible with the IBM 360 computer system.

C. CALCULATION OF ENERGY DENSITY SPECTRA

In a particular finite segment of a wave record of length T_r, let $A(t_k)$ represent the time series of N discrete wave amplitudes which are spaced at intervals of time Δt. Then the time of each sample amplitude is

$$t_k = k \Delta t, \qquad k = 1,\ldots,N \qquad (12)$$

The record is transformed from the time domain to the frequency domain by the Fourier transform

$$\hat{A}(f_j) = \frac{1}{N} \sum_{k=0}^{N-1} A(t_k) \; e^{-2\pi i jk/N}, \; j = 0,\ldots,N-1 \qquad (13)$$

where $f_j = j \Delta f$ are the component frequencies

$\hat{A}(f_j)$ are the complex amplitudes of the f_j

and $i = \sqrt{-1}$

In the computer, this transform is accomplished by the IBM library subroutine HARM, which uses the fast Fourier transform algorithm developed by Cooley and Tukey (3), and requires that N be an integral power of 2.

$\hat{A}(f_j)$ is a two-sided amplitude spectrum where N/2 corresponds to the aliasing or Nyquist folding frequency, f_c, which is the highest frequency analyzed. If the wave record had component frequencies above f_c, the amplitudes of these frequencies would be aliased into the spectrum $\hat{A}(f_j)$. A Nyquist frequency of 128 Hz was selected on the basis of the analog filter

characteristics as discussed in section A. The Nyquist frequency determines the minimum sampling interval, Δt, by the relation

$$\Delta t = 1/2f_c \tag{14}$$

The energy density spectrum, $S(f_j)$ is given by

$$S(f_j) = \frac{2 \left| \hat{A}(f_j) \hat{A}^*(f_j) \right|}{\Delta f} , \quad j = 0,\ldots,N/2 \tag{15}$$

where $\hat{A}^*(f_j)$ is the complex conjugate of $\hat{A}(f_j)$ and the factor 2 accounts for the inclusion of only half of the two-sided symmetrical amplitude spectrum. The $S(f_j)$ represent the average energy per unit frequency in an elementary frequency band of width Δf centered on f_j.

The $S(f_j)$ of one realization of an ergodic random process is a set of statistics, each of which is considered to have the Chi-square distribution with two degrees of freedom. The number of degrees of freedom determines the confidence limits for a statistic, and a meaningful comparison of statistics requires that the range of confidence limits be sufficiently small. The relation between the number of degrees of freedom and the confidence limits for the Chi-square distribution is given by Pierson and Marks (8).

An accepted method of increasing the confidence in the statistical estimate of energy density is to average a number, M, of elementary frequency bands into a wider equivalent band of width B_e. When this is done, each bandwidth B_e has 2M degrees of freedom. As the two degrees of freedom in each elementary bandwidth reflect two independent samples in the time domain, the record length, T_r, required for the analysis is then specified by:

$$T_r = N \Delta t = 2 f_c M \Delta t / B_e \tag{16}$$

Obviously, the increased confidence is bought at the expense of definition.

The parameters used for analysis of the wave records collected on 21 November 1968 are summarized as follows:

T_r = 64 seconds

N = 16384

Δt = 1/256 seconds

f_c = 128 Hz

B_e = 0.5 Hz

M = 32

For 64 degrees of freedom, the 95% confidence limits are 1.5 and 0.7, which means that for an infinite number of realizations of this particular wave process, 95% of the realizations of the spectrum would fall between 1.5 $S(f_j)$ and 0.7 $S(f_j)$.

In the discussion of the results of the spectral analyses in the following section, confidence limits have been omitted for clarity, but their existence must be recognized. In fact, the computed $S(f_j)$ are the most likely values.

VI. RESULTS AND IMPLICATIONS OF SPECTRAL CALCULATIONS

In the text and figures of the discussion that follows, the time (hours:minutes:seconds) assigned to a spectrum is the mid-time of the 64-second wave record from which the spectrum was derived. For the wind data subset of data sets A and B, refer to Figures 4 and 5, respectively.

A. COMPARISON OF SIMULTANEOUS UPWIND AND DOWNWIND SPECTRA

Figure 7 shows the energy density spectra computed from simultaneous realizations at the upwind and downwind wave probe positions at 11:55:56 and 11:57:00. This comparison implies that spectra from downwind probe data may be underestimated by a factor of approximately two. The most obvious cause for this under-estimation is an error in calibration; however, it is possible that the difference may be an effect of the geometry of the lake.

B. ATTENUATION INDICATED BY DATA SET A

Figure 8 shows the energy density spectra at the upwind probe position at 11:57:00 when the average wind at the eight foot level had been four knots or more for at least 30 minutes, and at the downwind probe position 112, 176, and 240 seconds later. During the four-minute interval represented, the wind diminished to 1.3 knots.

In the development of the generalized attenuation function earlier in this paper, the true energy density spectra at the generation and propagation positions were related by:

$$S(f,x) = S(f,0)\ \ k(x,\theta,f)\ \ G(f,x) \qquad (1)$$

and the attenuation function was specified by:

$$G(f,x) = e^{-mx} \qquad (11)$$

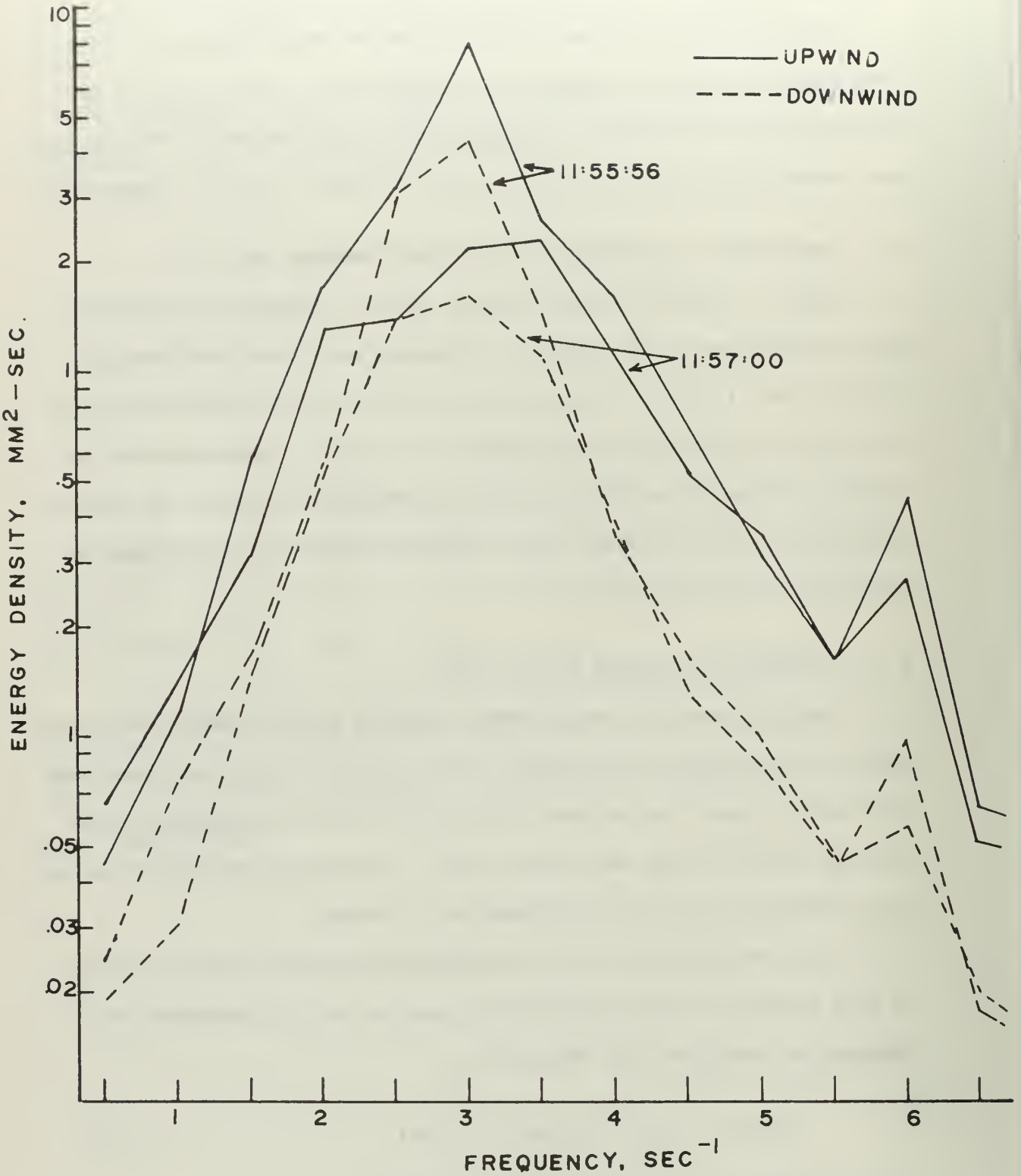

FIGURE 7. COMPARISON OF SIMULTANEOUS SPECTRA

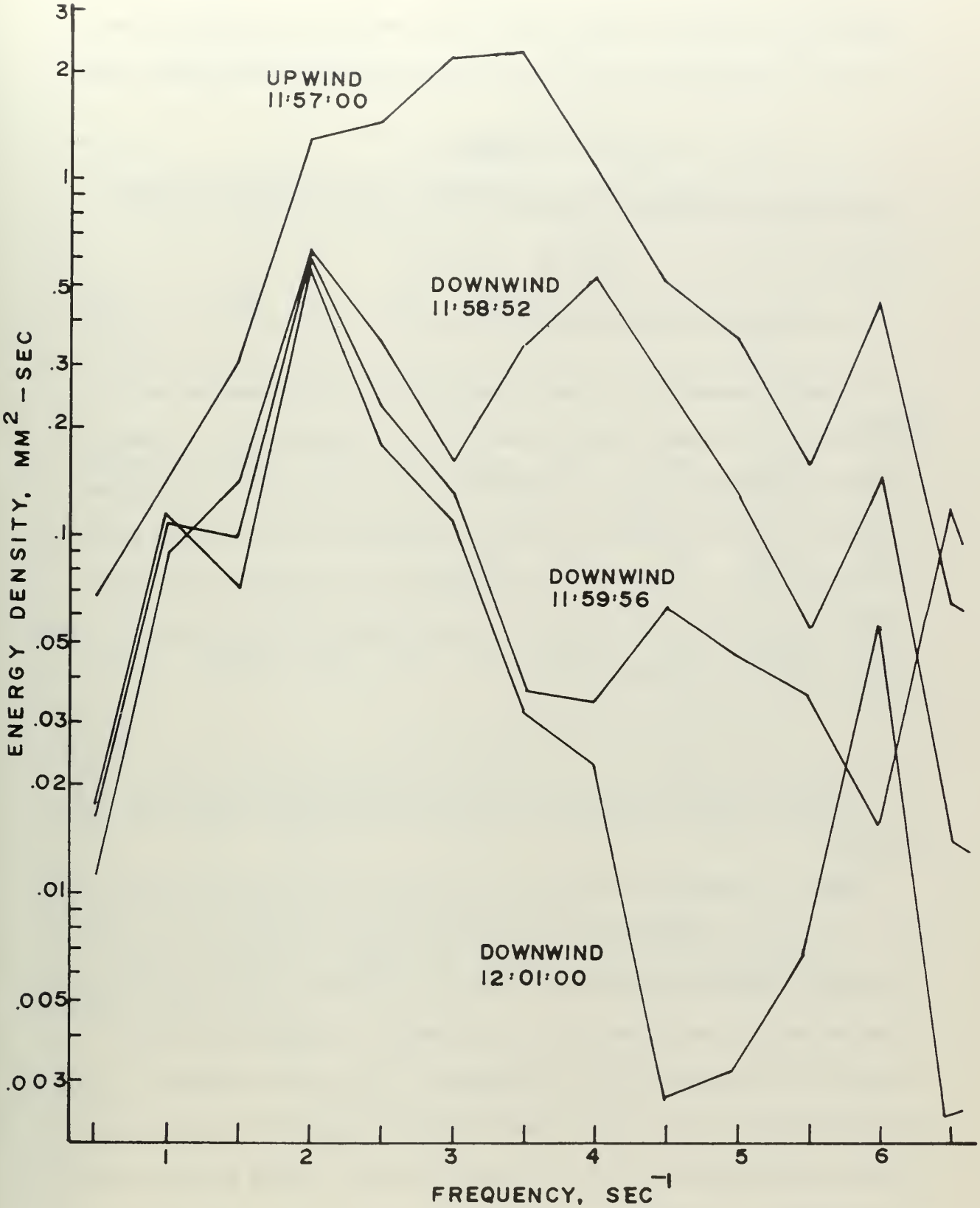

FIGURE 8. ENERGY DENSITY SPECTRA — DATA SET A

If it is assumed that the energy density spectra, $S(f_j,0)$ and $S(f_j,x)$, derived from measurements of the upwind and downwind probe positions, respectively, are equivalent to the continuous spectra, then

$$G(f,x) = \frac{S(f_j,x)}{S(f_j,0)\ k(x,\theta,f)} = e^{-mx} \qquad (17)$$

which, as the attenuation coefficient, $m = m(f)$, is sought, can be written:

$$m(f_j) = \frac{\ln\left[\dfrac{S(f_j,0)\ k(x,\theta,f)}{S(f_j,x)}\right]}{x} \qquad (18)$$

A valid comparison of energy densities for the determination of $m(f_j)$ can only be made when the identical wave components are present at both measurement points. Therefore, $S(f_j,0)$ measured at the upwind probe can only be compared with $S(f_j,x)$ measured at the downwind probe after the time, t, required for the energy of the component frequency f_j to propagate over the distance x, the effective distance between probes. This is given for gravity waves by

$$t = x / V_g = 4 \times \pi f / g \qquad (19)$$

where V_g is the group velocity of the f_j and g is the acceleration of gravity.

Table 1 summarizes the data and computations for $m(f_j)$ for data set A. As the $S(f_j)$ were computed at specific times, the frequencies whose propagation times corresponded to the time intervals between upwind and downwind spectra were computed by the inverse of equation (19) and rounded to the nearest ½ Hz to correspond to the center frequency of the band represented by f_j, unless the calculated frequency fell midway between center frequencies, then rounding was done in both directions and dual calculations made.

The second calculation of $m(f_j)$ under each frequency uses 2 $S(f_j,x)$ in place of $S(f_j,x)$ to show the effect of the possible error in the downwind spectra mentioned in section A.

TABLE 1

SUMMARY OF STATISTICS AND ATTENUATION COEFFICIENTS FOR DATA SET A

Upwind time	Downwind time	t sec	x ft	f_j sec^{-1}	$S(f_j,0)$ mm^2/Hz	$k(x,\theta,f)$	$S(f_j,x)$ mm^2/Hz	$m(f_j)$ ft^{-1}
11:57:00	11:58:52	112	138	2.0	1.31	.95	.648	.00473
								-.000348
11:57:00	11:59:56	176	138	3.0	2.24	.95	.136	.0199
								.0149
				3.5	2.35	.95	.0349	.0301
								.0251
11:57:00	12:01:00	240	138	4.5	.519	.95	.00265	.0377
								.0327

Now, as $m = m(f)$, assume that $m(f)$ can be expressed by the equation

$$m(f) = K f^p \tag{20}$$

where K is an attenuation constant and p is an integer.

Table 2 shows the values of K for the values of m(f) given in Table 1 for p = 2,3,4.

TABLE 2

ATTENUATION CONSTANTS FOR DATA SET A

f sec^{-1}	m(f) ft^{-1}	m(f) nm^{-1}	p = 2 K sec^2/nm	p = 3 K sec^3/nm	p = 4 K sec^4/nm
2.0	.00473	28.4	7.1	3.55	1.77
	-.000348	-2.08	-.52	-.26	-.13
3.0	.0199	119.	13.4	4.41	1.47
	.0149	89.3	9.9	3.31	1.10
3.5	.0301	180.	14.7	4.18	1.20
	.0251	150.	12.2	3.49	1.00
4.5	.0377	226	11.1	2.46	.545
	.0327	196	9.6	2.13	.472

C. COMPARISON WITH OCEAN SWELL DATA

Some energy density spectra of recorded Pacific Ocean swell from fetches at known distances from the swell observation point were made available by Wickham (12). Values of m and K for these data have been computed in the manner prescribed for these same values in Tables 1 and 2 above, and are displayed in Table 3. The data for Table 3 may include situations in which the winds in the propagation areas were across or opposed to the direction of propagation, where the data for Tables 1 and 2 were for only the following wind situation.

TABLE 3

ATTENUATION COEFFICIENTS AND CONSTANTS FOR OCEAN WAVES

f	m(f)	p = 2	p = 3	p = 4
sec^{-1}	nm^{-1}	K sec^2/nm	K sec^3/nm	K sec^4/nm
.105	.00275	.275	2.75	27.5
.095	.00224	.248	2.62	27.5
.095	.00261	.289	3.04	32.0
.085	.00266	.369	4.34	51.0
.075	.00378	.670	8.95	120.
.055	.00115	.380	6.93	125.

D. RESULTS OF DATA SET A AND TABLE 3

1. The possible error of a factor of 2 between spectra as discussed in section A. does not have a significant effect on the determination of attenuation for data set A. With the exception of the values at f_j = 2.0 Hz, the attenuation coefficients, m(f) are all of the same order of magnitude; and with the exception of the negative value for the second estimate of K for 2.0 Hz, the attenuation constants for each power of frequency are of the same order of magnitude.

2. If multiplying $S(f_j, x)$ by 2 had a small effect, then variations within the confidence limits for the spectral estimates will also have small effect.

3. It is quite evident that if an attenuation function can be described over a wide range of frequencies by a simple relationship such as proposed by equation (20), then it must be a function of f^3.

E. DATA SET B

The wind in data set B died more slowly than the dramatic change which allowed the extended calculations for data set A. For those short time periods where the wind declined rapidly, $S(f_j)$ were computed and are displayed in Figures 9, 10, and 11. As each figure represents only one attenuation observation, the corresponding values of $m(f_j)$ and K are shown on the figures.

Less confidence is placed in the results of data set B, as the results are more erratic and the spectra seem to be influenced near the frequencies of interest by a low frequency disturbance that is not evident in data set A. This low frequency could have been due to a surge set up in the lake by the gusting of the wind during its decline.

F. ADDITIONAL OBSERVATIONS

The persistence of the energy density at 2.0 Hz is interesting, especially in view of the negative values obtained when 2 $S(f_j,x)$ is substituted for $S(f_j,x)$ for the calculation of $m(f_j)$ and K. These negative values indicate that the energy in that particular frequency may be increasing with distance. A possible cause for this is that 2 Hz may be a low enough frequency to suffer negligible attenuation in such a short distance.

The second peak that occurs in both data sets at 6 Hz is also noteworthy. Possible explanations for this are that a frequency of 6 Hz is beginning to be influenced by surface tension effects, or the effect may be a result of non-linear interactions as have been reported by Pierson (7).

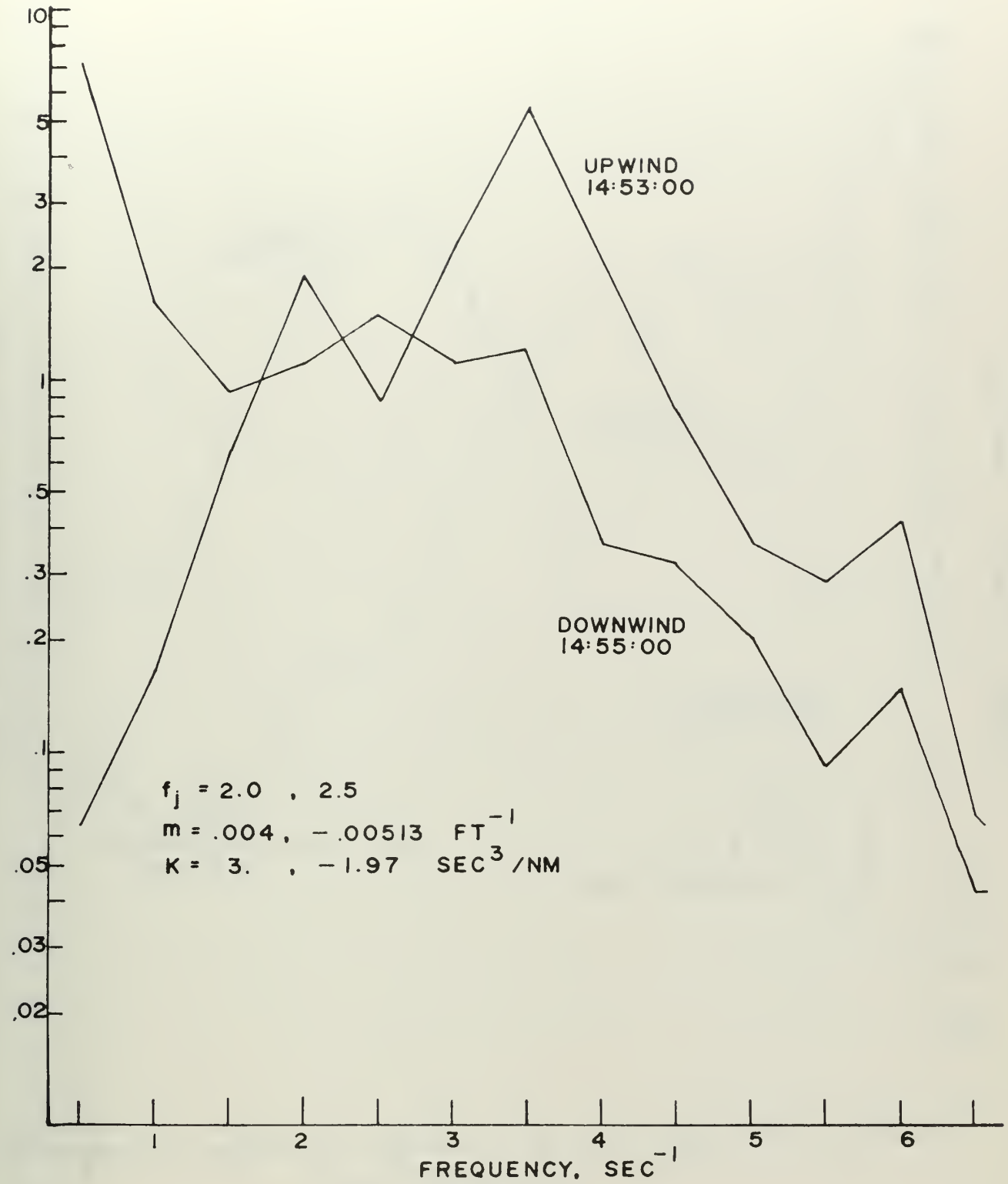

FIGURE 9. ENERGY DENSITY SPECTRA — DATA SET B

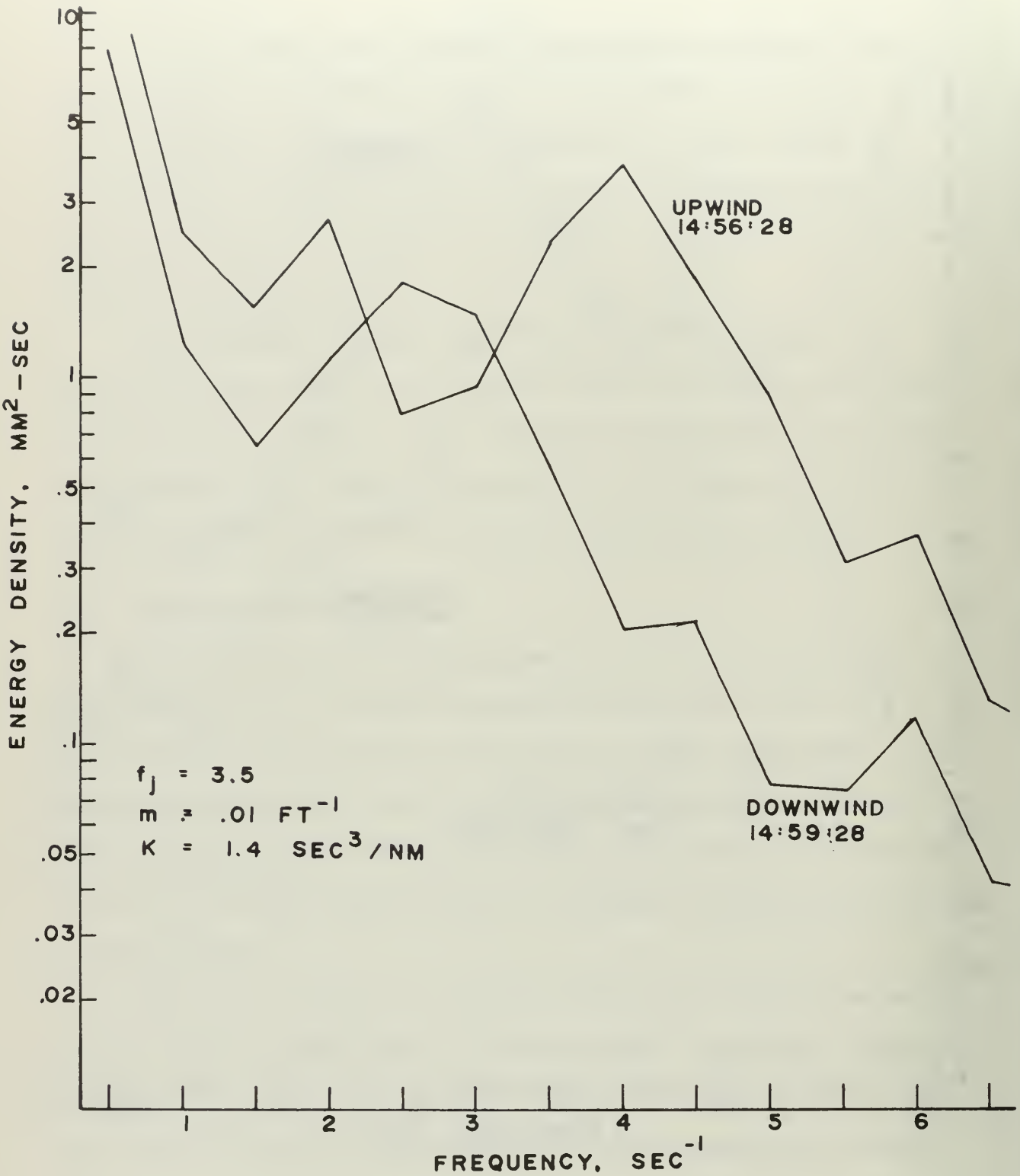

FIGURE 10. ENERGY DENSITY SPECTRA – DATA SET B

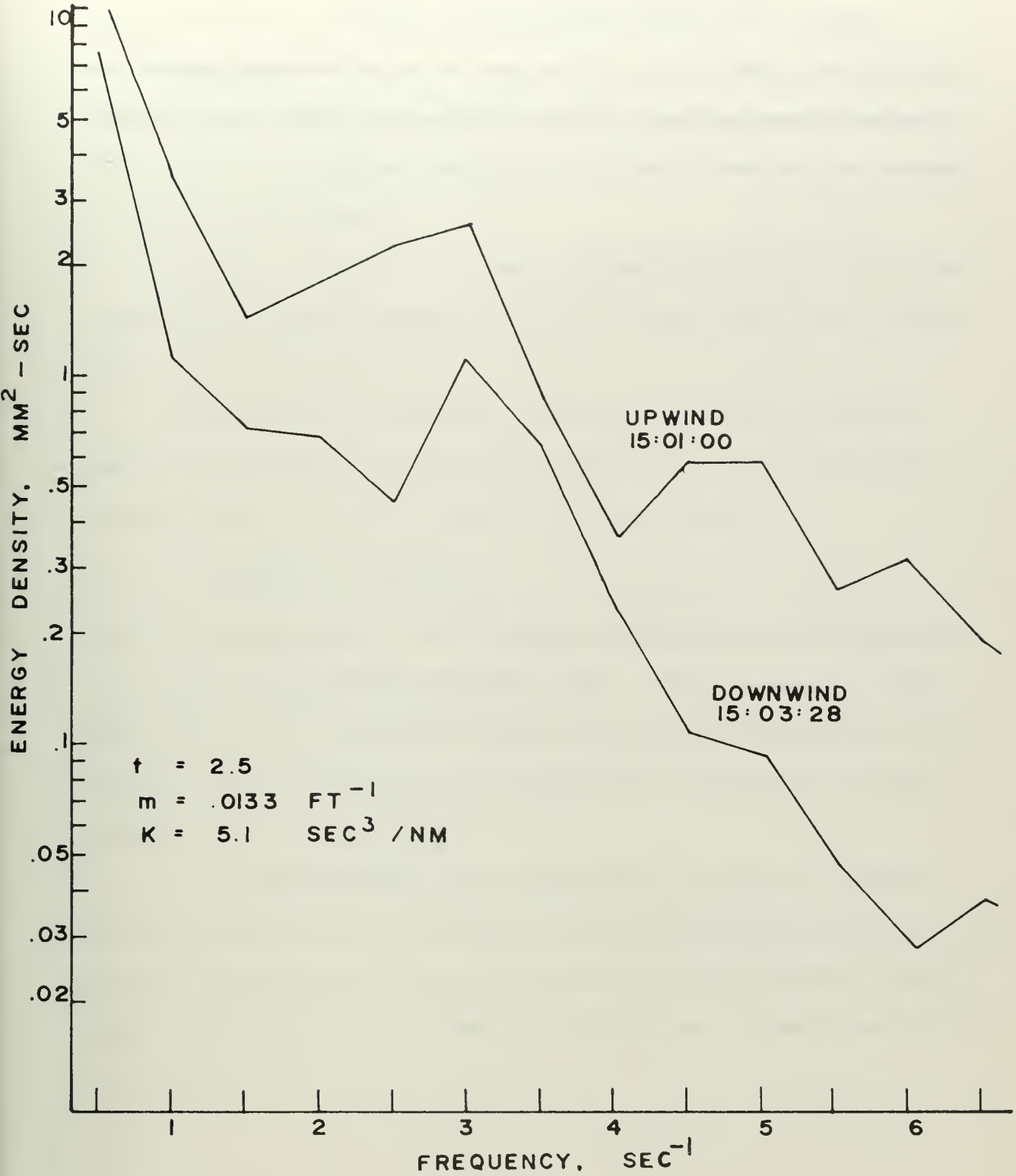

FIGURE 11. ENERGY DENSITY SPECTRA – DATA SET B

The decision to establish the Nyquist frequency at 128 Hz was not unwarranted, as examination of the spectra beyond the water surface wave frequencies show occasions of significant energy, particularly around 60 Hz.

VII. CONCLUSIONS AND RECOMMENDATIONS

The instrumentation, recording, filtering, digitizing and analytical techniques employed in support of this investigation were extremely effective in providing well defined energy density spectra from waves in a small scale environment.

The dying wind situation gives a definable separation of wind wave generation and swell propagation for high frequency waves when the wind dies rapidly and smoothly.

Strong evidence is provided in support of a contention that an empirical attenuation function can be applied to a wide range of frequencies, and it is proposed that this function might be

$$G(f,x) = e^{-Kf^3x}$$

where K is approximately 3 sec^3/nm for following winds and may increase to as much as 8 sec^3/nm for opposing winds. Future extensive investigation may show the frequency exponent to not be an integer, but for the current state of definition of the attenuation function this integral representation is satisfactory.

It is recommended that further studies be undertaken to provide better definition of such an empirical attenuation function, with emphasis placed on intermediate frequencies between the high frequencies investigated in this paper and the lower frequencies more frequently studied in the ocean.

BIBLIOGRAPHY

1. Barber, N. F., and F. Ursell. The Generation and Propagation of Ocean Waves and Swell. Phil. Trans. Roy. Soc. A, Vol. 240, pp. 527-560. 1948.

2. Cartwright, D. E., Modern Studies of Wind-Generated Ocean Waves. Contemp. Phys., Vol. 8, No. 2, pp. 171-183. 1967.

3. Cooley, James W., and John W. Tukey. An Algorithm for the Machine Calculation of Complex Fourier Series. Mathematics of Computations, Vol. 19, No. 90, p. 297. April 1965.

4. Darbyshire, J., Attenuation of Swell in the North Atlantic. Quar. J. Roy. Met. Soc., Vol. 83, 357, pp. 351-359. July 1957.

5. Pearlman, Michael J., Dynamic Calibration of Wave Probes. Massachusetts Institute of Technology, Department of Naval Architecture and Marine Engineering. Prepared under M.I.T. Contract No. DSR 6913. Sponsored by The Society of Naval Architects and Marine Engineers. Undated.

6. Phillips, O. M., The Dynamics of Random Finite Amplitude Gravity Waves. Ocean Wave Spectra. Proceedings of a Conference at Easton, Maryland, May 1-4, 1961. Englewood Cliffs, New Jersey, Prentice-Hall, Inc., pp. 171-189. 1963.

7. Pierson, Willard J., Some Nonlinear Properties of Long-Crested Periodic Waves with Lengths of Near 2.44 Centimeters. J. Geo. Res., Vol. 66, No. 1, pp. 163-179. January 1961.

8. Pierson, Willard J., and Wilbur Marks. The Power Spectrum Analysis of Ocean-Wave Records. Transactions, American Geophysical Union, Vol. 33, No. 6, p. 384. December 1952.

9. Pierson, Willard J., Gerhard Neumann, and Richard W. James. Practical Methods for Observing and Forecasting Ocean Waves by Wave Spectra and Statistics. H. O. Publication 603, U. S. Navy Hydrographic Office. 1955.

10. Post, Jerry Lee. Analysis and Synthesis of a Time Limited Complex Wave Form. Thesis. Naval Postgraduate School. December 1968.

11. Snodgrass, F. E., G. W. Groves, K. F. Hasselman, G. R. Miller, W. H. Munk, and W. H. Powers. Propagation of Ocean Swell Across the Pacific. Phil. Trans. Roy. Soc. A, Vol. 259, pp. 431-497. 1966.

12. Wickham, J. B., Naval Postgraduate School. Personal communication.

INITIAL DISTRIBTUION LIST

		No. Copies
1.	Defense Documentation Center Cameron Station Alexandria, Virginia 22314	20
2.	Library Naval Postgraduate School Monterey, California 93940	2
3.	Prof. J. B. Wickham Department of Oceanography Naval Postgraduate School Monterey, California 93940	6
4.	LCDR M. S. Carswell, USN Staff, Commander Destroyer Squadron TWO FPO New York 09501	1
5.	Officer in Charge Fleet Numerical Weather Facility Naval Postgraduate School Monterey, California 93940	1
6.	Oceanographer of the Navy The Madison Building 732 N. Washington Street Alexandria, Virginia 22314	1
7.	Naval Oceanographic Office Attn: Library Washington, D. C. 20390	1
8.	National Oceanographic Data Center Washington, D. C. 20390	1
9.	Naval Weather Service Command Washington Navy Yard Washington, D. C. 20390	1
10.	Director, Coast and Geodetic Survey Department of Commerce Attn: Office of Oceanography Washington, D. C. 20235	1
11.	Director, Maury Center for Ocean Sciences Naval Research Laboratory Washington, D. C. 20390	1

12. Office of Naval Research 1
Attn: Undersea Warfare (Code 466)
Department of the Navy
Washington, D. C. 20390

13. Office of Naval Research 1
Attn: Director, Surface and Amphibious Programs
(Code 463)
Department of the Navy
Washington, D. C. 20360

14. Mr. R. L. Limes, Supervisor 1
Electrical Engineering Deparment Computer Laboratory
Naval Postgraduate School
Monterey, California 93940

15. Prof. J. J. Von Schwind 1
Department of Oceanography
Naval Postgraduate School
Monterey, California 93940

16. Department of Oceanography (Code 58) 3
Naval Postgraduate School
Monterey, California 93940

DOCUMENT CONTROL DATA - R & D

Security classification of title, body of abstract and indexing annotation must be entered when the overall report is classified)

1 ORIGINATING ACTIVITY (Corporate author)	2a. REPORT SECURITY CLASSIFICATION
Naval Postgraduate School Monterey, California 93940	Unclassified
	2b. GROUP None

3 REPORT TITLE

Attenuation of Surface Waves in Deep Water

4 DESCRIPTIVE NOTES *(Type of report and inclusive dates)*

5 AUTHOR(S) *(First name, middle initial, last name)*

Michael Stuart Carswell

6 REPORT DATE	7a. TOTAL NO. OF PAGES	7b. NO. OF REFS
December 1968	47	12

8a. CONTRACT OR GRANT NO	9a. ORIGINATOR'S REPORT NUMBER(S)
N/A	N/A
b. PROJECT NO	
c.	9b. OTHER REPORT NO(S) *(Any other numbers that may be assigned this report)*
d.	

10 DISTRIBUTION STATEMENT

Distribution of this document is unlimited

11. SUPPLEMENTARY NOTES	12. SPONSORING MILITARY ACTIVITY
	Naval Postgraduate School Monterey, California 93940

13 ABSTRACT

The concept, instrumentation, and analytical techniques for the investigation of attenuation of wind generated water surface waves in a small scale real environment by separation of generation and propagation by time in the dying wind situation were developed, and an empirical attenuation function applicable to a wide range of frequencies proposed.

14 KEY WORDS	LINK A		LINK B		LINK C	
	ROLE	WT	ROLE	WT	ROLE	WT
Resistance Wave Meter						
Digital Analysis						
Fast Fourier Transform						
Wave Attenuation						
Attenuation Coefficient						